

## 弱電導性乱流のサブグリッドモデル

# A subgrid model of electrically conducting turbulent shear flows at low magnetic Reynolds number

下村 裕

東大理

Yutaka Shimomura<sup>1</sup>

Faculty of Science, University of Tokyo

## I. OBJECT

The objective of the present paper is to study by using LES technique how the magnetic field influences the detailed structures of MHD turbulent channel flows, such as each component of the turbulent energy. In this case, it is natural to suppose that we should incorporate the effect of magnetic fields into the SGS model as in the  $k - \epsilon$  model. So, in the present paper, we propose a new SGS model of weakly-conducting turbulent shear flows, and demonstrate its superiority to the usual SGS model, or the Smagorinsky model, by comparing their results with laboratory experiment.

In II, we formulate LES in MHD at low magnetic Reynolds number  $R_m$  version, present a new SGS model for it, and apply it to a channel flow configuration. In III, the results of the present SGS model are compared with those of the Smagorinsky model, and the former are found to be closer to the experimental observation than the latter. Finally in IV, our conclusions are summarized.

---

<sup>1</sup>Present address: Department of Physics, Keio University, 4-1-1 Hiyoshi, Kohoku-ku, Yokohama 223, Japan

## II. FORMULATION

### A. Governing equations for the large-scale fields

A system of filtered equations for grid-scale (GS) components of incompressible MHD flows at low magnetic Reynolds number<sup>1</sup> is given by

$$\frac{\partial}{\partial t} \bar{u}_i + \frac{\partial}{\partial x_j} (\bar{u}_j \bar{u}_i) = -\nabla \bar{p} + \nu \nabla^2 \bar{u}_i + \frac{\sigma}{\rho} ((-\nabla \bar{\varphi} + \bar{\mathbf{u}} \times \mathbf{B}_0) \times \mathbf{B}_0)_i +$$

$$\frac{\partial}{\partial x_j} (R_{ij} + L_{ij} + C_{ij}), \quad (1)$$

$$\nabla \cdot \bar{\mathbf{u}} = 0, \quad (2)$$

$$\nabla^2 \bar{\varphi} = \nabla \cdot (\bar{\mathbf{u}} \times \mathbf{B}_0) = \mathbf{B}_0 \cdot \bar{\boldsymbol{\omega}}, \quad (3)$$

where the SGS Reynolds stress  $R_{ij}$ , the Leonard stress  $L_{ij}$ , and the cross correlation  $C_{ij}$  are given by the same definitions as in the usual non-conducting case since Lorentz force is linear at low  $R_m$  with regard to the velocity  $\mathbf{u}$ ; namely,

$$R_{ij} = -\overline{u_i'' u_j''}, \quad (4)$$

$$L_{ij} = \bar{u}_i \bar{u}_j - \overline{\bar{u}_i \bar{u}_j}, \quad (5)$$

$$C_{ij} = -(\overline{\bar{u}_i u_j''} + \overline{u_i'' \bar{u}_j}). \quad (6)$$

We should keep in mind that in (1) and in the following, the repeated subscripts are summed from 1 to 3 unless an exception is mentioned.

### B. Subgrid-scale modeling

In order to close the filtered equations (1)-(3), we need SGS modelings for  $R_{ij}$ ,  $L_{ij}$ ,  $C_{ij}$ . For non-conducting flows, the Smagorinsky model<sup>2</sup> is usually adopted for  $R_{ij}$ , while both  $L_{ij}$  and  $C_{ij}$  are often neglected. This modeling is shown to work well, and conserves Galilean invariance as pointed out by Speziale.<sup>3</sup> In MHD case, however, the validity of this modeling is questionable since no effects of magnetic fields are explicitly incorporated into it. Especially, it is obvious that we can not keep the Smagorinsky model valid in the laminar state appearing under the strong magnetic field: even in the laminar state, the SGS eddy viscosity does not diminish where the GS flow has large spacial variation.

Here, let us construct a SGS model of MHD turbulent shear flows at low  $R_m$  in the light of the author's previous study.

The author<sup>4,5</sup> showed theoretically that at the level of ensemble average, the usual eddy-viscosity representation of the Reynolds stress should be modified by the effect of magnetic field. Based on the modified representation of the Reynolds stress, a new  $k - \epsilon$  (two-equation) model including this effect was proposed, and it was demonstrated by comparing the numerical and experimental data that the new  $k - \epsilon$  model is better than the existing one in explaining the laminarization by the strong magnetic field. In this work, it was noticed that the most crucial effect of magnetic fields on turbulence appears as the negative contribution to the eddy viscosity. So, we modify by analogy the representation of the SGS Reynolds stress in the form of negative eddy viscosity as follows:

$$R_{ij} = -\frac{1}{3}\overline{u_a''u_a''}\delta_{ij} + \nu_{SGS}\bar{e}_{ij}, \quad \bar{e}_{ij} = \left( \frac{\partial \bar{u}_i}{\partial x_j} + \frac{\partial \bar{u}_j}{\partial x_i} \right), \quad (7)$$

$$\nu_{SGS} = \nu_e + \nu_m, \quad (8)$$

$$\nu_e = C_0 \epsilon_{SGS}^{1/3} \Delta^{4/3}, \quad \nu_m = -\frac{\sigma}{\rho} C_1 \Delta^2 |\mathbf{B}_0|^2. \quad (9)$$

In (7),  $\delta_{ij}$  is the Kronecker delta symbol, and  $\nu_{SGS}$  is the total SGS eddy viscosity which is composed of the two parts  $\nu_e$  and  $\nu_m$  in (8):  $\nu_e$  is the familiar positive SGS eddy viscosity involved in turbulence, and  $\nu_m$  is the negative one caused by magnetic fields. In (9),  $C_0$  and  $C_1$  are model constants theoretically evaluated as

$$C_0 \sim 0.04, \quad C_1 \sim 0.03, \quad (10)$$

$\epsilon_{SGS}$  is the SGS energy dissipation rate defined by

$$\epsilon_{SGS} = \nu \frac{\partial u_a''}{\partial x_b} \frac{\partial u_a''}{\partial x_b}, \quad (11)$$

and  $\Delta$  is the representative length scale of the form

$$\Delta(x, y, z) = (\Delta x \Delta y \Delta z)^{1/3}, \quad (12)$$

where  $\Delta x$ ,  $\Delta y$ , and  $\Delta z$  denote the computational mesh sizes in the  $x$ ,  $y$ , and  $z$  directions, respectively.

Next, following the way<sup>6</sup> of deriving the Smagorinsky model of non-conducting turbulence, we assume the balance of SGS energy production and dissipation rate; namely,

$$R_{ij} \frac{\partial \bar{u}_i}{\partial x_j} = \epsilon_{SGS} + \frac{\sigma}{\rho} C_2 \epsilon_{SGS}^{2/3} \Delta^{2/3} |\mathbf{B}_0|^2. \quad (13)$$

The second term on the right-hand side of (13) shows the additional SGS energy dissipation of conducting turbulence due to Lorentz force, and the

model constant  $C_2$  is theoretically estimated as

$$C_2 \sim 0.4. \quad (14)$$

Now, we are ready to express the total SGS eddy viscosity  $\nu_{SGS}$  in terms of GS variables. The substitution of (7)-(9) into (13) leads to the equation for  $\epsilon_{SGS}$ , which is solved in a perturbational manner on the assumption that the terms including  $|\mathbf{B}_0|^2$  are small. As a result of this procedure, we get the expression of  $\nu_{SGS}$  as

$$\nu_{SGS} = \nu_s - \frac{\sigma}{\rho}(C_m\Delta)^2|\mathbf{B}_0|^2, \quad (15)$$

$$\nu_s = (C_s\Delta)^2 \left( \frac{1}{2}\bar{e}_{ab}\bar{e}_{ab} \right)^{1/2}, \quad (16)$$

where

$$C_s = C_0^{3/4} \sim 0.09, \quad C_m = \frac{1}{\sqrt{2}}(3C_1 + C_0C_2)^{1/2} \sim 0.2. \quad (17)$$

Here we should note, as is clear from the derivation, this expression is valid only for weak magnetic fields. So, we extend (15) to the following formula available for strong magnetic fields:

$$\nu_{SGS} = \nu_s \exp \left( -\frac{\sigma}{\rho}(C_m\Delta)^2|\mathbf{B}_0|^2/\nu_s \right). \quad (18)$$

This expression asymptotically agrees with (15) when the magnetic field is weak, and further guarantee the positiveness of total SGS eddy viscosity in its diminishing process under the strong magnetic field. Of course, the SGS model (18) reduces to the familiar Smagorinsky model  $\nu_s$ , when the electrical conductivity  $\sigma = 0$ . In (18), the effect of magnetic field on turbulence is introduced in the form of damping factor which is locally determined.

As is usually done for the LES of non-conducting turbulence, we also introduce the wall damping function to explain low-Reynolds-number effects on the SGS Reynolds stress near the wall;  $\Delta$  is multiplied by the wall damping function  $f$  of Van Driest type,<sup>7</sup> which is given in case that the wall is located on the  $z = 0$  plane by

$$f(z^+) = 1 - \exp\left(-\frac{z^+}{A^+}\right), \quad A^+ = 25, \quad (19)$$

In (19)  $z^+$  is the distance to the nearest wall in the wall units, and it is defined by the friction velocity  $u_\tau$  as

$$z^+ = \frac{zu_\tau}{\nu}, \quad u_\tau = \left(\nu \frac{\partial \langle \bar{u}_1 \rangle}{\partial z} \Big|_{z=0}\right)^{1/2}, \quad (20)$$

where  $\langle \bar{u}_1 \rangle$  denotes the ensemble mean of the streamwise GS velocity.

We complete the SGS modeling (7), (16), (18), and (12) multiplied by the wall damping function (19) with the assumption

$$L_{ij} = 0, \quad C_{ij} = 0. \quad (21)$$

In the present simulation, the model constants are chosen as

$$C_s = 0.1, \quad C_m = 1.4. \quad (22)$$

The value 0.1 of the Smagorinsky constant  $C_s$  is usually used for non-conducting turbulence, and close to the predicted value 0.09 in (17) as shown by Yoshizawa.<sup>6</sup> On the other hand, the optimized value 1.4 of  $C_m$  does not agree with the theoretically estimated value 0.2 in (17). The reason of this disagreement is not clear now. For weak magnetic fields, the damping factor due to magnetic field in (18) might not make a major contribution to  $\nu_{SGS}$ : the SGS eddy

viscosity (18) might work only for stronger magnetic fields. In this sense, the derivation of SGS model is never perfect, but in the present paper, we report favorable features of the present SGS model in comparison with the Smagorinsky model  $\nu_{SGS} = \nu_s$ .

The equations (1)-(3) for the GS fields with the SGS modeling described above constitute the basic system of equations to be solved in the present numerical simulation of MHD turbulent shear flows at low  $R_m$  under a uniform magnetic field.

### C. Magnetohydrodynamic channel flows under a uniform magnetic field

We study MHD turbulent plane channel flows at low  $R_m$  under a uniform magnetic field which is normal to the walls.

The flow configuration and the coordinate system used in this paper are shown in Fig. 1. Here,  $x$ ,  $y$ , and  $z$  denote the streamwise, spanwise, and normal ( to the wall ) directions, respectively;  $u_1$ ,  $u_2$ , and  $u_3$  are the velocity components along  $x$ ,  $y$ , and  $z$ , respectively. The origin  $O$  of the normal coordinate,  $z = 0$ , is located on the bottom wall. A magnetic field of magnitude  $B_0$  is uniformly applied in the direction of positive  $z$  to the conducting fluid between two horizontal walls, which are separated each other at the distance of  $L$ . We suppose that the walls are insulated and its streamwise and spanwise dimensions ( $L_x$  and  $L_y$ , respectively) are supposed to be infinite compared with the channel whole width  $L$ .

## III. RESULTS

In this section, we show the results of the present SGS model. They are compared with those of the Smagorinsky model and the experimental data of Brouillette and Lykoudis.<sup>8</sup> All simulations for various Hartmann numbers are done with the same fixed  $Re = 29000$ . For each case, the governing equations are integrated forward in time until the solutions reach the statistically steady state. This steady state is identified by an approximate time-independence of the horizontally averaged GS component of streamwise velocity. After the statistically steady state is attained, horizontal averages of various quantities are moreover averaged in time period  $t = 64$  for which the equations are further integrated. In the following,  $\langle \cdot \rangle$  means the time and horizontal ( $x - y$ ) average.

## A. Comparison with the Smagorinsky model

Figure 2 shows the skin friction coefficients

$$C_f = \frac{u_\tau^2}{U_0^2/2} = -L \frac{\partial \langle \bar{P} \rangle}{\partial x} / U_0^2, \quad (23)$$

as a function of  $H_a/Re$ . The solid line indicates the laminar result deduced from Hartmann's analytical solution; namely

$$C_f = 2 \frac{H_a}{Re} \{ \coth(H_a/2) - 2/H_a \}^{-1} \\ \sim 2 \frac{H_a}{Re} \quad (H_a \gg 1). \quad (24)$$

The symbols  $\bullet, \circ, \times$  mean the the experimental data of Brouillette and Lykoudis<sup>8</sup>, the calculation based on the Smagorinsky model, and the calculation based on the present model. The experimental data approach the



laminar solution as  $H_a/Re$  increases. Compared with the experimental data, the Smagorinsky model gives too small  $C_f$  at  $H_a/Re \sim 1.8 \times 10^{-3}$ , and too large at  $H_a/Re \geq 4.3 \times 10^{-3}$ . Both deficiencies come from the same reason that the SGS eddy viscosity under a magnetic field is too large in the Smagorinsky model. At  $H_a/Re \sim 1.8 \times 10^{-3}$ , the large SGS eddy viscosity suppresses GS turbulence and the momentum in the middle of the channel can not diffuse so much to the wall, which leads to the small  $C_f$ . At  $H_a/Re \geq 4.3 \times 10^{-3}$ , the fluctuation is almost diminished by the GS Lorentz force so that  $C_f$  is roughly determined by the formula  $C_f \sim 2H_a/Re^*$ , where  $Re^* = U_0L/(\nu + \nu_{SGS})$ . Consequently, too large  $\nu_{SGS}$  results in too large  $C_f$ . The present model saves these deficiencies by introducing the damping effect of magnetic fields in the SGS eddy viscosity, and gives  $C_f$  closer to the experimental data both at  $H_a/Re \sim 1.8 \times 10^{-3}$  and at  $4.3 \times 10^{-3}$ .

In the following Figs. 3 and 4, couples of figures (a) and (b) are compared with each other: the results of the Smagorinsky model are shown in (a), and those of the present model in (b).

Figure 3 shows the mean streamwise velocity profiles  $\langle \bar{u}_1^+ \rangle$  at  $H_a = 0, 52.5$ , and  $125$ . At  $H_a = 0$ , the calculated profiles in both figures are the same, and approximately satisfy in the logarithmic region

$$\langle \bar{u}_1^+ \rangle = (1/0.41) \ln z^+ + 5.5, \quad (25)$$

where  $z^+$  is given by (20) and  $\bar{u}_1^+ \equiv \bar{u}_1/u_\tau$ . The predicted constants 0.41 (von Kármán) and 5.5 are very close to the generally accepted value 0.4 and  $5.0^{9,10}$  for non-conducting wall turbulence. At  $H_a = 52.5$  and  $H_a = 125$ , the calculated profiles are compared with the corresponding experimental data

of Brouillette and Lykoudis<sup>8</sup> shown by the symbol  $\square$  and  $\triangle$ . By the same reason described in Fig. 2, the profiles predicted by the Smagorinsky model are far from the experimental data while the present model shows fairly good agreements. So, the present model properly predicts local quantities as well as the global one such as  $C_f$  in Fig. 2.

Figure 4 plots the profiles of GS turbulence intensities of velocity fluctuations  $\bar{u}'_1$ ,  $\bar{u}'_2$ , and  $\bar{u}'_3$  at  $H_a = 0, 40$ , and  $52.5$ . They are normalized by  $u_\tau$  and contrasted with the experimental data of Kreplin and Ecklemann<sup>11</sup> at  $H_a = 0$ . At  $H_a = 0$ , the computational peak value of  $\langle \bar{u}'_1{}^2 \rangle^{1/2}$  is slightly larger and that of  $\langle \bar{u}'_3{}^2 \rangle^{1/2}$  is just lower than the experimental data. Similar defect is also reported in the computation of Horiuti.<sup>12</sup> However, the agreements are fairly well with regard to  $\langle \bar{u}'_2{}^2 \rangle^{1/2}$ . Comparing (a) with (b), we notice that the magnetic field laminarizes the GS turbulence faster in the Smagorinsky model than in the present model. The difference is most outstanding at  $H_a = 52.5$ : near the wall, the GS turbulence intensities of velocity fluctuations almost vanish in (a), but survive in (b). As was explained in Fig. 2, this difference gives rise to the drastic change of skin friction coefficient at  $H_a/Re \sim 1.8 \times 10^{-3}$ . Judging from better agreements of the present model with the experiment on the skin friction coefficients and the mean streamwise velocity profiles in Figs. 2 and 3, the data in Fig. 4 (b) is more reliable than in Fig. 4 (a). In Fig. 4 (b), we should notice the anisotropy in the laminarization process around  $z = 0.03$  ( $z^+ \sim 40$ ) where the intensity  $\langle \bar{u}'_1{}^2 \rangle^{1/2}$  takes its peak value: the difference of  $\langle \bar{u}'_1{}^2 \rangle^{1/2}$  between three cases is very small compared with those of  $\langle \bar{u}'_2{}^2 \rangle^{1/2}$  and  $\langle \bar{u}'_3{}^2 \rangle^{1/2}$ .

## IV. CONCLUSIONS

LES technique is used to study the effects of a uniform magnetic field on MHD turbulent channel flows. We propose a new SGS model into which the effect of magnetic field is incorporated in the form of local damping factor for SGS eddy viscosity. It is assured that the new model shows better agreement than the Smagorinsky model with the available experimental data of the skin friction coefficients and the mean streamwise velocity profiles.

The new model predicts the detailed structures of magnetohydrodynamic turbulent channel flows, which is beyond the power of the approach based on such one-point global turbulence models as  $k - \epsilon$  model. Especially, the anisotropic laminarization of turbulence by the magnetic field is quantitatively clarified: near the wall,  $\langle \bar{u}_1'^2 \rangle^{1/2}$ ,  $\langle \bar{e}_2'^2 \rangle^{1/2}$ , and  $\langle \bar{e}_3'^2 \rangle^{1/2}$  are not so influenced by the magnetic field as the other components of the intensities  $\langle \bar{u}_2'^2 \rangle^{1/2}$ ,  $\langle \bar{u}_3'^2 \rangle^{1/2}$ , and  $\langle \bar{e}_1'^2 \rangle^{1/2}$ .

## REFERENCES

- <sup>1</sup>U. Schumann, J. Fluid Mech. **74**, 31 (1976).
- <sup>2</sup>J. W. Deardorff, J. Fluid Mech. **41**, 453 (1970).
- <sup>3</sup>C. G. Speziale, J. Fluid Mech. **156**, 55 (1985).
- <sup>4</sup>Y. Shimomura, J. Phys. Soc. Jpn. **57**, 2365 (1988).
- <sup>5</sup>Y. Shimomura, J. Phys. Soc. Jpn. **57**, 4453 (1988).
- <sup>6</sup>A. Yoshizawa, Phys. Fluids **25**, 1532 (1982).
- <sup>7</sup>E. R. Van Driest, J. Aeronaut. Sci. **23**, 1007 (1956).
- <sup>8</sup>E. C. Brouillette and P. S. Lykoudis, Phys. Fluids **10**, 995 (1967).

<sup>9</sup>A. K. M. F. Hussain and W. C. Reynolds, *J. Fluids Eng.* **97**, 568 (1975).

<sup>10</sup>H. Tennekes and J. L. Lumley, *A First Course in Turbulence* (MIT Press, Cambridge, MA 1972), p.149.

<sup>11</sup>H. Kreplin and M. Ecklemann, *Phys. Fluids* **22**, 1233 (1979).

<sup>12</sup>K. Horiuti, *J. Comput. Phys.* **71**, 343 (1987).

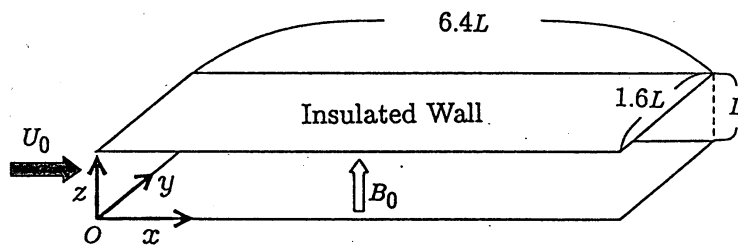


FIG. 1. Flow configuration and coordinate system.

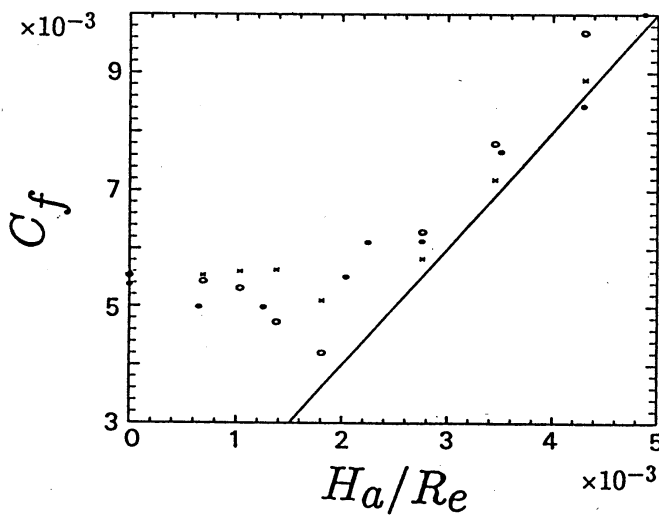


FIG. 2. Skin friction coefficients  $C_f$ :  
 o, Smagorinsky model; •, experimental data of Brouillette and Lykoudis ;  
 ×, present model; —, laminar line ( $C_f = 2H_a/R_e$ ).

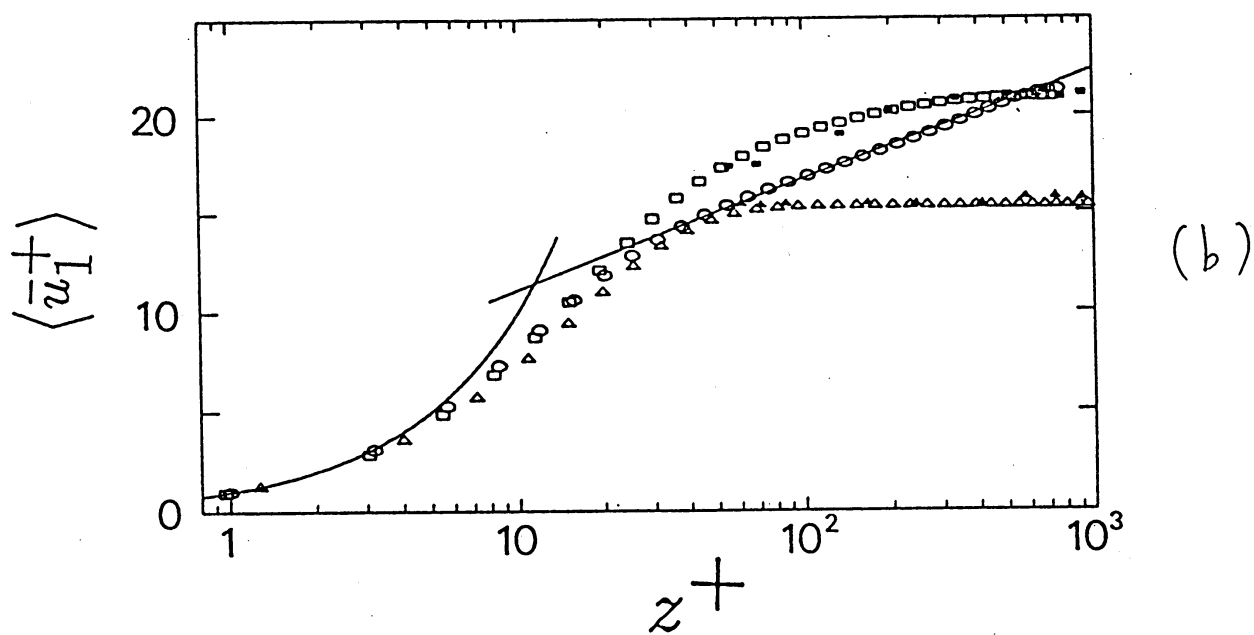
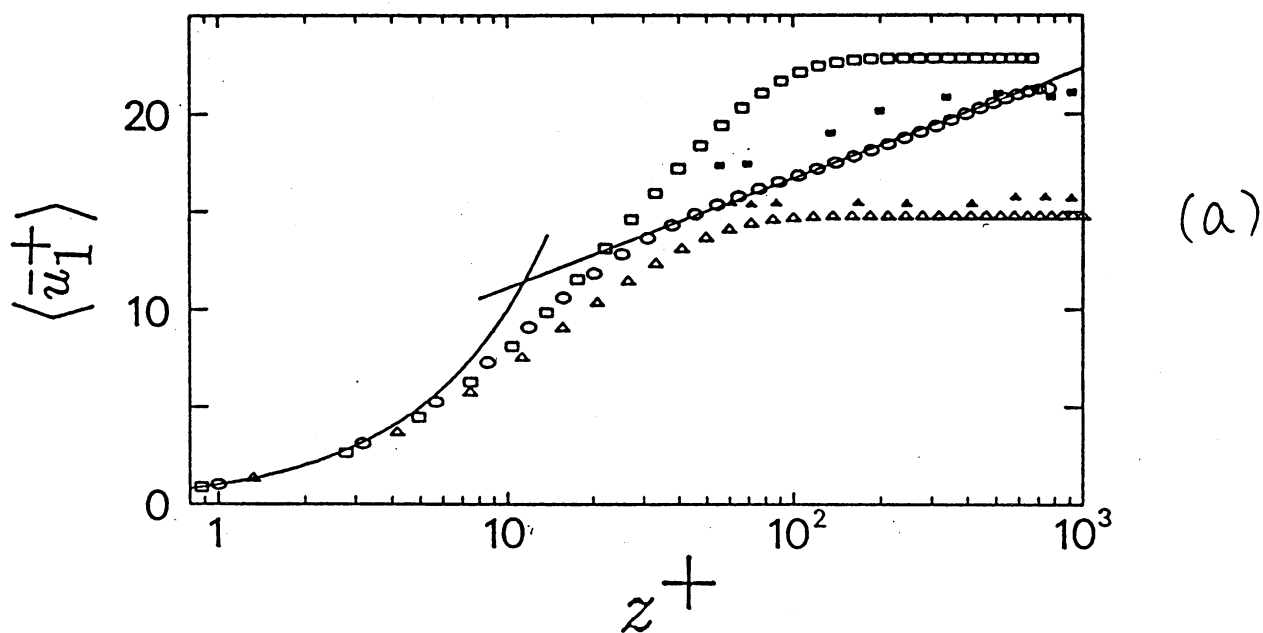


FIG. 3. Mean streamwise velocity profiles  $\langle \bar{u}_1^+ \rangle$ :  $\circ$ ,  $H_a = 0$ ;  $\square$ ,  $H_a = 52.5$ ;  $\triangle$ ,  $H_a = 125$ ;  $\blacksquare$ , experimental data of Brouillette and Lykoudis at  $H_a = 52.5$ ;  $\blacktriangle$ , experimental data of Brouillette and Lykoudis at  $H_a = 125$ ; —,  $\langle \bar{u}_1^+ \rangle = z^+$  ( $z^+ \leq 10$ ) and  $\langle \bar{u}_1^+ \rangle = (1/0.41) \ln z^+ + 5.5$  ( $z^+ \geq 10$ ).

(a) Smagorinsky model; (b) present model.

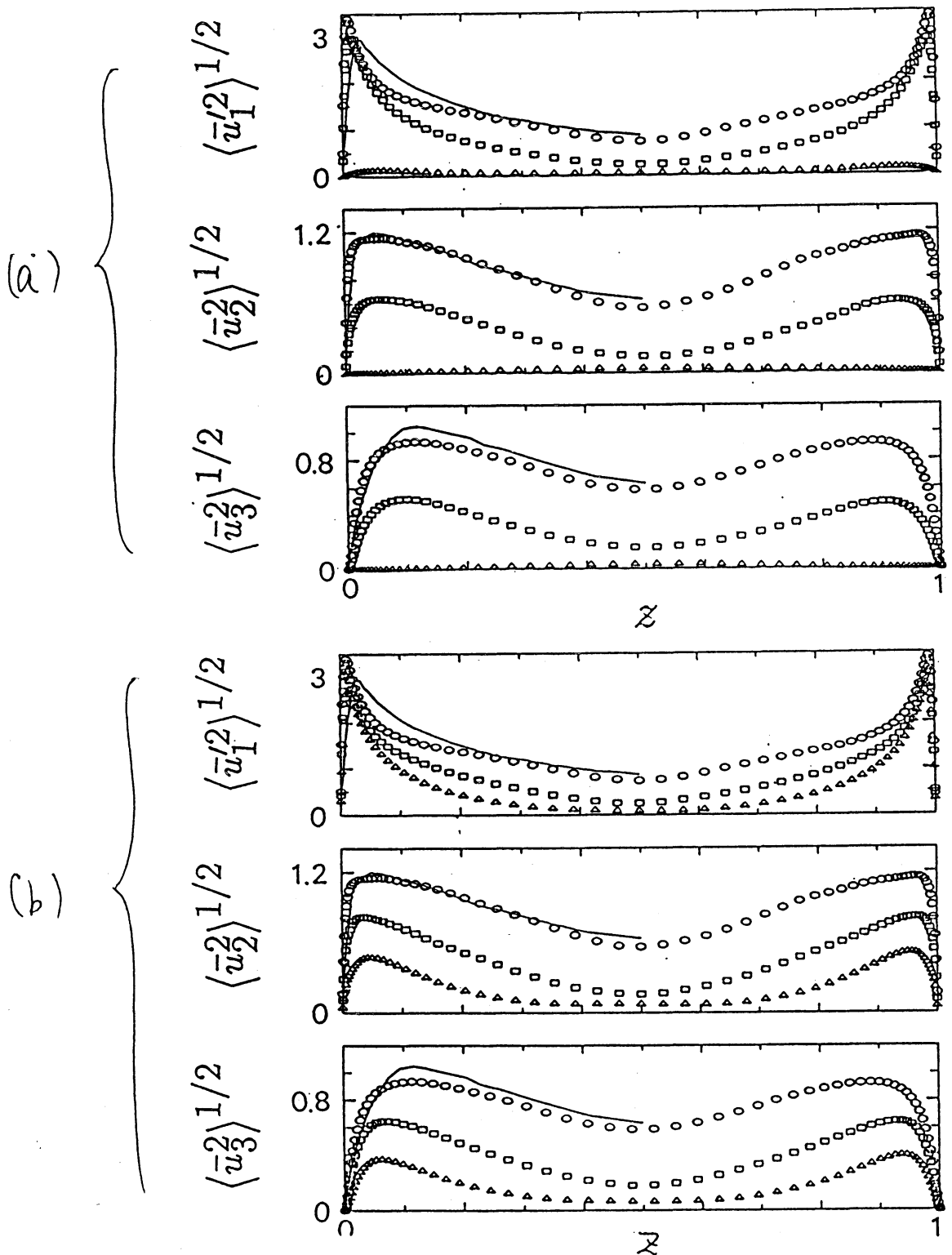


FIG. 4. GS-intensities of the velocity fluctuations:  $\bigcirc$ ,  $H_a = 0$ ;  $\square$ ,  $H_a = 40$ ;  $\triangle$ ,  $H_a = 52.5$ ; —, experimental data of Kreplin and Ecklemann at  $H_a = 0$ .

(a) Smagorinsky model; (b) present model.